Preferential Transport of Soil Colloidal Particles: Physicochemical Effects on Particle Mobilization

M. Rousseau, L. Di Pietro, R. Angulo-Jaramillo,* D. Tessier, and B. Cabibel

ABSTRACT

The quantification of particle transport through soil is of great importance for estimating the potential risk of adsorbing contaminants leaching into groundwater. In the present study, we investigated the mobilization of natural soil particles in an undisturbed soil column (diameter = 0.3 m, height = 0.66 m). We tested the effects of physicochemical properties of soil and infiltrating water on the mobilization and transport of soil particles. A square pulse of water was applied at the top of the column. Water was allowed to drain freely at the bottom of the column. We tested two rainfall intensities (11 and 23 mm h^{-1}), three ionic strengths (10^{-5}, 10^{-3}, and 10^{-1} *M*), and two initial moisture contents (0.34 and 0.38 m^3 m^{-3}). For the whole set of infiltration experiments, the concentration of eluted particles was correlated with the drainage flow intensity, particularly during transient flow. Particle leaching during steady flow varied with the boundary and initial conditions. The highest mobilization of particles was observed for deionized water, the highest infiltration rate and the highest initial soil moisture content. Particle mobilization was limited for high ionic strength associated with the divalent cation Mg^{2+}. During transient flow, mechanical detachment by hydrodynamic shear could lead to particle mobilization. During steady flow, the ionic strength of the incoming solution may alter the energy potential at the soil–water interface, and thus have an effect on the mobilization rate as well.

In the last few decades, it has been shown that colloidal particles transported through the soil may contribute to the accumulation of low-solubility contaminants in groundwater (McCarthy, 1989; Ryan and Elimelech, 1996; Kretzschmar et al., 1999). The unexpectedly rapid transport of cationic radionuclides (Pu, Am) that has been observed at hazardous waste sites has been attributed to colloid-facilitated transport (Champ et al., 1982; Travis and Nuttall, 1985; Penrose et al., 1990). The transport of heavy metals (Kaplan et al., 1995; Jensen and Christensen, 1999) and highly adsorbing pesticides (Worrall et al., 1999) has also been explained by this mechanism. The quantification of particle transport through soil is therefore of great importance for estimating the potential risk of adsorbing contaminants leaching into groundwater.

A large number of studies have addressed these problems. Most of the experimental studies were performed on repacked soil (Gruesbeck and Collins, 1982; Wan and Wilson, 1994b; Roy and Dzombak, 1997; Grolimund et al., 1998; Gamerdinger and Kaplan, 2001a), or artificial porous media (Elimelech and O'Melia, 1990; Wan and Wilson, 1994a; Silliman, 1995; Roy and Dzombak, 1996). These studies consisted of laboratory infiltration experiments after injection of colloidal particles (latex microspheres, polystyrene latex particles with specified functional groups, in situ mobilized soil colloidal particles, or pure silica) into the topsoil. Only a few were performed on undisturbed soil columns where naturally occurring particles were collected (Kaplan et al., 1993; Jacobsen et al., 1997; Laegdsmand et al., 1999; Schelde et al., 2002). Some field studies have also shown that rainfall events could lead to the leaching of a certain quantity of particles in drainage water (Pilgrim and Huff, 1983; Grant et al., 1996; Jarvis et al., 1999; Laubel et al., 1999; Worrall et al., 1999).

The mobilization of particles in soils is affected by the water flow regime. Kaplan et al. (1993) showed that increasing rainfall intensity could increase the concentration of particles in the effluent from undisturbed soil cores. The authors suggested that particles were primarily mobilized by shear stress on the macropore walls, and hypothesized that a relationship may exist between the shear stress intensity and the kinetic energy of the water flowing through the effective porosity. Other experimental studies have shown that high rainfall intensities increase the transport velocity of particles injected at the soil surface (Vilks and Bachinski, 1996; Harter et al., 2000).

The rapid transport of particles to depth depends on the structure of the soil, particularly on the presence of vertical continuous macropores. Pilgrim and Huff (1983), Jacobsen et al. (1997), Laegdsmand et al. (1999), Laubel et al. (1999), and McKay et al. (2000) observed rapid breakthrough of colloidal particles involving preferential flow. Pilgrim and Huff (1983) as well as Hardy et al. (2000) suggested that the particles were detached at or near the soil surface by raindrop impact and that subsurface flow subsequently carried the particles primarily through soil macropores. The results of tracer and dye experiments supported the hypothesis of preferential flow through vertical continuous macropores (Jacobsen et al., 1997; Laegdsmand et al., 1999).

The composition of the soil, the stability of its structure and the chemistry of the soil–water system are also determinant factors in the detachment and mobilization of soil particles. For example, the effect of ionic strength of the incoming solution on particle mobilization was investigated: (i) in artificial porous media (Elimelech and O'Melia, 1990; Roy and Dzombak, 1996; Kretzschmar

M. Rousseau, L. Di Pietro, and B. Cabibel, Institut National de la Recherche Agronomique–Unité Climat, Sol et Environnement, Domaine St. Paul, 84914 Avignon Cedex 9, France; M. Rousseau and R. Angulo-Jaramillo, Laboratoire d'étude des Transferts en Hydrologie et Environnement, Domaine Universitaire, B.P. 53, 38041 Grenoble Cedex 9, France; D. Tessier, Institut National de la Recherche Agronomique–Unité de Science du Sol, Route de Saint Cyr, 78026 Versailles Cedex, France. Received 14 February 2003. Original research article. *Corresponding author (angulo@hmg.inpg.fr).

Published in Vadose Zone Journal 3:247–261 (2004).

677 S. Segoe Rd., Madison, WI 53711 USA

Abbreviations: DDL, double diffuse layer; FWHM, full width at half maximum; TOC, total organic C; XRD, X-ray diffraction.

et al., 1997), (ii) in homogeneous repacked soil columns (Fauré et al., 1996; Roy and Dzombak, 1997; Saiers and Hornberger, 1999; Gamerdinger and Kaplan, 2001a, 2001b), and (iii) in undisturbed structured soils (Kaplan et al., 1996; Laegdsmand et al., 1999). All of these experiments showed that lower ionic strength enhanced the release of particles. Fauré et al. (1996) and Kretzschmar et al. (1997) found an ionic strength threshold below which particles started to be released. The value of the threshold depended on the porous medium.

The presence of divalent cations (Ca^{2+}, Mg^{2+}) enhances the deposition process, whereas monovalent cations (Na^{+}, K^{+}) act as a dispersant (Elimelech and O'Melia, 1990; Kaplan et al., 1996; Roy and Dzombak, 1996; Kretzschmar and Sticher, 1997; Grolimund et al., 1998). Changes in solution chemistry promote colloid mobilization mainly by altering the double layer potential energy (Ryan and Elimelech, 1996). When the thickness of the hydrodynamic boundary layer is much greater than the thickness of the region influenced by the intersurface potential energy, colloid release is postulated to be a two-step mechanism in which either detachment from the surface or diffusion across the boundary layer can control the overall release rate. Colloid release is limited by detachment when a potential energy barrier is present, and by diffusion when the energy barrier is removed by a change in solution chemistry (Ryan and Gschwend, 1994).

Transport of particles also depends on the water distribution within the soil. Wan and Wilson (1994a, 1994b) showed that the gas–water interface preferentially sorbs colloidal particles relative to the solid–water interface under simulated groundwater conditions. Once adsorbed onto the interface, some particles can be desorbed by chemistry or shear stress. Wan and Tokunaga (1997) proposed a film-straining theory, which suggests that transport of suspended colloids can be retarded due to physical restrictions imposed by thin water films in partially saturated porous media (validated through transport of hydrophilic latex particles in sand columns).

Little is known about the effect of the initial soil moisture content on the mobilization of particles. Gamerdinger and Kaplan (2001a) showed that decreasing water content resulted in increased colloid deposition. This suggests that a portion of the favorable sites for deposition is associated with the excluded or immobile water domain and is not accessible to colloids.

Few studies are concerned with decreasing and replenishing the pool of dispersible particles during and between rainfall events (Worrall et al., 1993, 1999; Grant et al., 1996; Schelde et al., 2002). According to these field studies, pool replenishment could be due to freeze–thaw cycles and drying. Grant et al. (1996) made correlations between particulate matter concentration and several meteorological parameters. They found that particle concentration was significantly correlated only to the amount of precipitation. Worrall et al. (1993) suggested that the concentration of suspended sediments declined exponentially with time during rainfall events. They hypothesized that the decrease in the supply of sediment could be due to sealing of the surface by crusts, blockage of macropores through which the sediment moves, and having a finite supply of breakable aggregates at the surface.

Schelde et al. (2002) showed that a seemingly unlimited source of in situ colloids exists even after prolonged leaching; they observed that the peak concentration of colloids in the effluent after flow interruption increased with increasing length of the preceding pause. Schelde et al. demonstrated that colloid mobilization is not controlled by hydrodynamic shear induced by the flowing water, but by a time-dependant and possibly diffusion-limited process. They hypothesized that two diffusion processes govern colloid release to the flowing water, one in a uniform water film lining the macropore and one in the crust of the macropore.

The size of naturally mobile particles ranges from 10^{-1} to 10 μm (Pilgrim and Huff, 1983; Kaplan et al., 1993; Degueldre et al., 1996; Kaplan et al., 1997). These mobile particles consist mainly of clay minerals (smectites, kaolinite, gibbsite), organic matter, and Fe-oxides/hydroxides (Ryan and Gschwend, 1990; Kretzschmar et al., 1993; Degueldre et al., 1996; Kaplan et al., 1997). Also, it has been shown that organic coatings on soil particles can modify (increase or decrease) the stability of colloids in suspension (Kretzschmar et al., 1995; Kretzschmar and Sticher, 1997). Furthermore, the high negative charge of colloids gives them a strong adsorption power, thus further favoring their potential role in colloid-facilitated contaminant transport (Artinger et al., 1998). The role of pH-dependent charges is also important since it determines the magnitude and ability to pollutants to be retained by sorption or complexation. Furthermore, heavy metals are also present in the structure of minerals and organic constituents (McBride, 1989). Some field experiments have shown that a peak in contaminant concentration often observed in drainage waters was correlated to a peak in total organic C (TOC) content at the beginning of the draining period. Worrall et al. (1999) for example observed this phenomenon for pesticide leaching.

Moreover, soil colloids are potentially reactive with respect to the sorption of chemical species due to their large specific surface area and the high number of functional groups. The ability to be suspended, the sorption capacity, the complexing behavior, and the presence of contaminants in their crystal structure (heavy metals) make colloids potential vectors for contaminant transport in soil.

Although the effect of each of the physicochemical parameters reviewed above has been tested on particle mobilization, no comprehensive sensitivity analysis of all of these parameters has been performed on the same undisturbed soil column. Hence, in the present study, we investigate the mobilization of soil particles in an undisturbed soil column. We focus on the role of macropores in preferential leaching of soil particles. We then analyze the effect of rainfall intensity, initial soil moisture content and ionic strength on the mobilization and transport of soil particles. Finally, we determine the temporal evolution of the macropore network and its interaction with particle mobilization.

Table 1. Chemical, physical, and mineralogical soil properties.

Horizon	H1	H2	H3	H4
Depth, cm	0–23	23–34	34–65	65–70
		Chemical properties		
Organic C, g kg^{-1}	9.34	4.80	4.28	2.97
$CaCO_3$, g kg^{-1}	2	<1	<1	222
PH	7.5	7.3	7.7	8.5
CEC, soil pH	12.1	12.3	12.6	13.6
Exchangeable Ca, cmol kg^{-1}	11.66	11.18	12.23	14.18
Exchangeable Mg, cmol kg^{-1}	0.83	0.56	0.53	0.28
Exchangeable K, cmol kg^{-1}	0.57	0.45	0.34	0.25
Exchangeable Na, cmol kg^{-1}	0.03	0.04	0.04	0.07
Free Fe, %	0.65	0.73	0.80	0.78
Ionic strength, mol L^{-1}	1.19×10^{-2}	7.51×10^{-3}	7.70×10^{-3}	1.99×10^{-2}
		Physical properties		
Clay, %	18.2	20.9	23.6	19.9
Loam, %	60.2	60.7	59.4	63.8
Sand, %	21.6	18.4	14	16.3
Bulk density, g cm^{-3}	1.56	1.54	1.47	1.50
Porosity, cm^3 cm^{-3}	0.41	0.42	0.44	0.43
Draining porosity, cm^3 cm^{-3}	0.027	0.038	0.030	0.019
Water content at saturation, cm^3 cm^{-3}	0.40	0.41	0.42	0.42
Hydraulic conductivity at saturation, m s^{-1}	1.70×10^{-5}	3.15×10^{-4}	4.20×10^{-4}	2.62×10^{-5}
		Mineralogical properties		
Chlorites, %	2.07	3.15	3.28	2.16
Smectites, %	25.86	45.84	30.82	70.89
Interstratified Illites/Smectites, %	8.62	6.29	0	11.86
Illites, %	50.69	37.30	54.10	8.89
Kaolinite, %	12.76	7.42	11.80	6.20

MATERIALS AND METHODS

Soil Properties

An undisturbed soil core (diameter = 0.3 m, height = 0.66 m) was extracted from the experimental field Les Closeaux (Versailles, France). The soil is a tilled loamy clay soil underlying loess deposits. The soil profile was divided into four layers on the basis of both textural and structural characteristics (Table 1). Soil samples of each soil layer were collected for soil characterization near where the soil column had been extracted. Relevant physical and hydraulic properties for each soil layer were determined using small undisturbed soil cores (diameter = 0.15 m, height = 0.07 m) extracted in the field. The physicochemical properties of the four layers are presented in Table 1. The first three layers contain mainly illites and smectites. The higher smectite content of the deepest horizon reflects a very different mineralogical composition due to clay migration by leaching during pedogenesis. To characterize the macroporosity and its temporal evolution, the soil core was scanned with an X-ray scanner (General Electric, Chicago, IL), which is a CAT scanner unit (Computer Assisted Tomography), before and after the infiltration experiments, at the Exploration Production Department of TotalFinaElf (Pau, France). Current and voltage of the X-ray beam were 300 mA and 140 kV, respectively. The exposure time was 2 s. The X-ray attenuation is dominated by Compton scattering, but is corrected by the scanner. A set of images, 3 mm thick every 3 mm with a resolution of 0.6 mm per pixel, was obtained. These settings produced images with satisfactory contrast between voids (air- or water-filled) and the soil matrix. Soil water content for the first and second scanning were nearly the same as indicated by TDR probes measurements.

A soil column vertical sleeve for a fixed radius before the infiltration experiments (two-dimensional reconstruction was obtained with TotalFinaElf's software) is given in Fig. 1a. Three-dimensional reconstruction of the macroporosity within the soil column (Fig. 1b) was obtained using a method presented in Pierret et al. (2002). Structural characteristics of the macropore networks were obtained using a procedure described by Capowiez et al. (1998).

Soil Column Experiments

Figure 2 shows a diagram of the experimental device used for the infiltration/drainage experiments through the soil column. A rainfall simulator consisting of 204 hypodermic needles, 0.5 mm in diameter, distributed in a 2.5-cm square network, supplied water at the top of the core. The hypodermic needles were about 30 cm above the soil surface, and produced a raindrop kinetic energy of about 10^{-5} J (with drop diameters of 2 mm), which is lower than that of natural rainfall (Salles and Poesen, 2000). The rainfall simulator rotated to allow a random distribution of raindrops, thus preventing the formation of depressions at the soil surface, which was not protected in any way. A pulsating pump controlled rainfall intensity and duration. The bottom of the core was positioned on a perforated Plexiglas plate onto which a funnel was sealed. The weight of the out-flowing solution during the experiments was recorded over a period of time. We estimated the drainage hydrograph for each experiment from these data. The effluent was sampled during and after each infiltration experiment, until draining stopped. To ensure a sufficient volume of leached particles in the percolate for analysis, the sampling frequency was varied from 3 to 10 min depending on the leaching rates.

Volumetric moisture contents and pressure heads within the column were recorded using six time domain reflectometry (located at 3, 15, 27, 45, 57, and 64 cm) and 12 tensiometers (located every 6 cm in the core), respectively (see Fig. 2).

A set of twelve infiltration experiments was performed on the same soil core (Table 2). Each infiltration consisted of the application of a square pulse of water of intensity q_0 and duration t_0 at the top of the core. Drainage was free at the bottom of the column. A steady-state draining flux was established for all infiltration experiments. Each experiment was performed after a draining period varying from 5 h to one

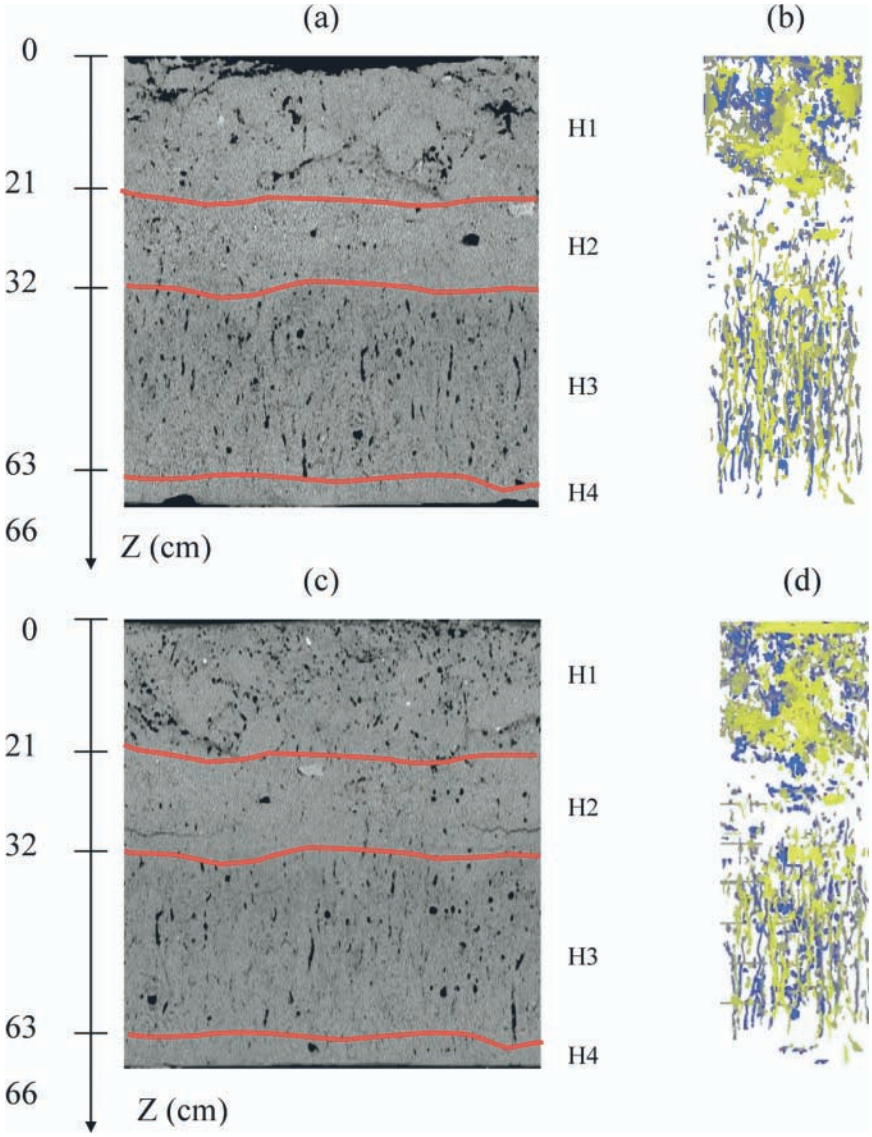

Fig. 1. (a) Two-dimensional soil column lagging for a fixed radius (reconstructed from X-ray tomography pictures) before infiltration experiments. (b) Three-dimensional reconstruction of the macropore network before the infiltration experiments. The network corresponds to the spatial distribution of porosity above a certain threshold, defined by the number of pixels necessary to build an object and the gray level intensity to distinguish soil matrix and porosity. The foreground is yellow and the background is blue. (c) Two-dimensional soil column lagging for a fixed radius after infiltration experiments. (d) Three-dimensional reconstruction of the macropore network after infiltration experiments.

month. All infiltration experiments took place over an 8-mo period. Two rainfall intensities were applied (11 and 23 mm h^{-1}), corresponding to naturally occurring storm events at the experimental site. These experiments were performed with deionized water. The ionic strength of the applied solution was then changed by adding $MgCl_2$ salt. Two ionic strengths were tested (10^{-3} and 10^{-1} M) while maintaining a constant rainfall intensity.

Except for Run 8, the initial water content of the column was set at field capacity (defined in this work as the water content after 1 wk of free drainage from saturation). According to the initial conditions of the experiments, it was assumed that flow occurred mainly in macropores. Run 8 was performed after only 5 h of drainage from saturation, under wetter initial conditions, to test the influence of initial soil moisture content on particle mobilization. A control experiment ($MgCl_2$ 10^{-3} M; 11 mm h^{-1}) was repeated three times, between other trials, to test the temporal evolution of naturally particles leached from the same soil column.

All combinations between rainfall intensity, ionic strength of applied solution and initial soil moisture content could not be tested since too many infiltration experiments on the same column would have produced changes in the soil hydraulic properties, thus compromising repeatability. Even if a different soil column had been used for each set of parameters, it would have been difficult to compare experiments because of structure variability.

A tracer experiment was performed with $MgBr_2$ to calculate the resident time in the column from the Br^- breakthrough curve and, therefore, to evaluate the extent of preferential flows. A pulse of 50 mL $MgBr_2$ (10^{-3} M) was applied at the soil surface during steady flow regime, for Runs 3 and 5. The composition of eluted samples was estimated by posterior analysis. To compare particle breakthrough curves resulting from different infiltration experiments, their evolution was plotted versus dimensionless time (t^*) to account for differences in breakthrough time (t_b) and infiltration duration (t_0).

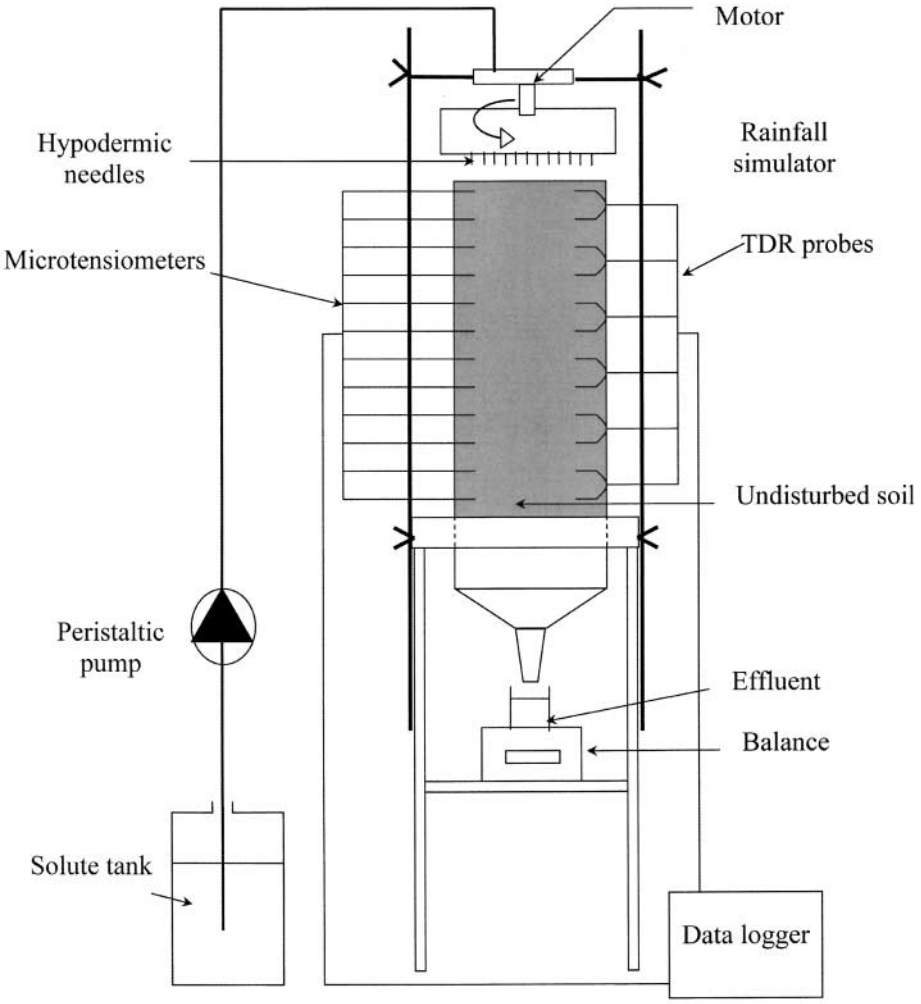

Fig. 2. Experimental set-up of the particle leaching experiments.

The chemical composition of eluted particles during infiltration was also plotted against t^*, which is defined as

$$t^* = \frac{t - t_b}{t_0 - t_b} \quad [1]$$

Effluent Analysis Methods

The particle concentration of the effluent was measured by light extinction at a wavelength of 400 nm with a UV/VIS spectrophotometer (551S, Perkin-Elmer). A correlation between naturally occurring particle concentration and light extinction was determined on several effluent samples ranging from the lowest to the highest concentration as detected with the spectrophotometer. The particle concentration for calibration was determined by weighing after drying at 60°C over a period of 24 h. A linear relationship between the light absorbance (DO) and particle concentration (C) in mg L^{-1} was used: $C = 312.24 \times DO$ ($R^2 = 0.99$). The relative uncertainty linked to solution sampling before the light extinction measurements was <5%.

The particle-size distribution was determined by laser diffraction. We used a Mastersizer 2000 laser grain-sizer with the Hydro 2000SM (A) accessory (Malvern Instruments, UK),

Table 2. Experimental conditions for all rainfall events performed on the soil column.

Rainfall event number†	Time after last rainfall event	Initial soil water content‡	Initial soil surface water content§	q_0	t_0	Influent nature	Influent ionic strength
		$m^3\ m^{-3}$		mm h^{-1}	min		mol L^{-1}
3	1 mo	0.34	0.32	10.98	228	$MgCl_2$	1.64×10^{-3}
4	1 wk	0.34	0.33	11.25	260	deionized water	7.02×10^{-6}
5	1 wk	0.36	0.34	11.13	225	$MgCl_2$	1.71×10^{-3}
6	1 wk	0.35	0.34	22.88	110	deionized water	1.25×10^{-5}
8	5 h	0.38	0.38	22.13	180	deionized water	1.57×10^{-5}
10	1 wk	0.34	0.34	10.94	185	$MgCl_2$	1.40×10^{-3}
12	1 wk	0.35	0.35	11.20	180	$MgCl_2$	1.30×10^{-1}

† Runs 1, 2, 7, 9, and 11 are not reported because technical hitch happened during these infiltrations. We decided to keep initial references of runs, to show infiltration history of the column.
‡ Average of soil water content at six depths of the column.
§ Soil water content given by the wave guide at a depth of 3 cm.

with a range of 0.02 to 2000 μm, in 100 fractions. Sizes were calculated using Mie's theory. We used water as a dispersant (refractive index = 1.33 at 20°C), and assumed the refractive index and absorption coefficient of natural particles to be 1.52 and 0.1, respectively. Effluent samples and the fine fraction (<2 μm) of the four soil horizons were analyzed for their clay mineralogy by X-ray diffraction (XRD) with a Siemens D5000 theta/2theta in reflection mode, using C_0K_α radiation, under 40 kV and 30 mA at a wavelength of 1.789 Å. We prepared oriented specimens by sedimentation on a glass slide and air-drying. For quantitative comparison, XRD patterns were interpreted using the DIFFRACT AT (Socabim Instruments, France) software. The XRD patterns were decomposed into their elementary component curves using the least-squares computer program DECOMPXR software (Lanson, 1993). This method was described in detail by Lanson (1997). The decomposition follows various stages. Initially, XRD patterns were recorded numerically by DECOMPXR, and their background effects eliminated. Gaussian or Lorentzian functions were used to identify elementary peaks. This method is a reliable tool to describe XRD patterns of minerals, as well as interstratified clay minerals (Lanson, 1997). A quantitative phase analysis was performed to determine relative surface peaks of clay minerals and interstratified minerals. The various minerals were then identified and quantified according to their peak intensity and the full width at half maximum (FWHM). The surface peak (%) is equal to FWHM versus intensity.

The TOC content of the effluent was determined with a TOC analyzer (5050A, Shimadzu) using a Pt catalyzer. Before TOC analysis, eluted samples were treated with 100 μL of NaN_3 (30 mg L^{-1}) in a 10-mL solution to inhibit microbiological activity. The Br^- concentration was analyzed using a Capillary Ion Analyzer (Waters, Milford, MA). The major cation concentration was analyzed by an Atomic Absorption Spectrometer (SpectrAA 2220, Varian). Before cation analysis, eluted samples were treated with 25 μL of HCl (1 *M*) in a 10 mL of solution to prevent oxidation–reduction reactions.

RESULTS AND DISCUSSION

Soil Structural Characteristics

Figures 1a and 1b show the initial macroporosity reconstruction. The macropores apparently consist of planar voids and cylindrical burrows. The first are probably cracks and the latter are probably earthworm channels or old root holes. Four layers exhibiting distinct structural characteristics can be distinguished.

The topsoil layer H1 (0–21 cm), with a high degree of macroporosity (0.031 m^3 m^{-3}), is mainly composed of cracks or voids created by soil tillage. The second layer, corresponding to the compacted tillage pan layer H2 (21–32 cm), shows a higher density with few macropores (0.004 m^3 m^{-3}). The third layer H3 (32–63 cm) exhibits a high degree of macroporosity (0.011 m^3 m^{-3}), probably due to earthworm burrows. The deeper layer H4 (63–66 cm) is very dense with few macropores (0.001 m^3 m^{-3}). Quantitative structural characteristics of the macropore networks given in Table 3 confirm these observations.

The structural characteristics of the soil column changed after 12 infiltration experiments (Table 3). The total macroporosity of the entire soil profile was reduced by 6% and that of the topsoil layer H1 by 19%. According to computed tomography pictures, some cracks in the topsoil layer disappeared or were partially clogged after infiltration trials (Fig. 1c,d). This could be explained by the swelling of clays and/or by clogging of some macropores by particles released from the topsoil. We could not directly quantify the shrinking and swelling of clays during infiltration. However, it seems likely that swelling was greater than particle deposition within the macropores (Michel et al., 2000).

However, the total number of macropores significantly increased after the series of infiltrations, both for the entire profile (an increase of 44%) and particularly in the topsoil layer H1 (an increase of 133%). Moreover, the mean length of the macropores decreased by 17% in the entire profile. From these quantitative results, it is reasonable to assume that some draining macropores lost their vertical continuity by being altered into two or more discontinuous macropores. Thus, it is likely that some changes in the macropore network connectivity occurred.

Hydrodynamic Behavior of the Soil Column

The drainage hydrograph curves are shown in Fig. 3. Since the plots are representative of the other curves, only hydrographs from Runs 4, 10, and 12 are presented. Three phases can be identified: a fast increase in the draining flux, a steady outflow rate, and a rapidly decreasing flux just after rainfall has stopped. Specific times define these phases: t_s is the time necessary to establish the steady flow rate and t_D is the arrival time of the draining front at the bottom of the soil column (see Fig. 3). Two time intervals, T1 and T2 (the transient periods during the rising and the falling hydrogram, respectively), were then calculated as the difference between t_s and t_b and the difference between t_D and t_0, respectively, to characterize the length of time of the transient periods at the beginning and at the end of the rainfall (Table 4).

Figure 4a shows a rapid increase in the capillary pres-

Table 3. Structural characteristics of 3D reconstructed macropore network before and after infiltration experiments.

		Macroporosity		Number of macropores		Mean height of macropores†	
Horizon	Depth	Before	After	Before	After	Before	After
	cm	cm^3 cm^{-3}				cm	
Entire profile	1.2–66	0.016	0.015	850	1221	1.91	1.59
H1	1.2–21.3	0.031	0.025	255	595	1.29	1.26
H2	21.3–32.7	0.004	0.005	108	97	1.32	1.01
H3	32.7–63	0.011	0.012	478	459	2.36	2.18
H4	63–66	0.001	0.001	4	4	0.68	0.8

† The height is calculated as the difference in depth between the bottom and the entry of the macropore.

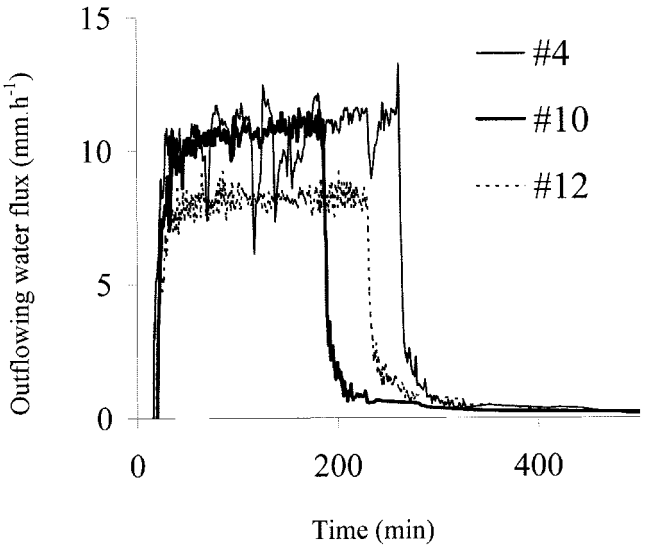

Fig. 3. Drainage hydrographs for rainfall events 4, 10, and 12.

sure just after infiltration starts. Some tensiometers in the deepest horizon seemed to respond earlier than others in the upper horizons (e.g., the capillary pressure at 66 cm increased before the pressure at 39 cm). This could be due to preferential flow; however, tensiometric data are a very local measurement and do not provide reliable means of visualizing nonuniform wetting fronts. Nevertheless, Fig. 4b confirms these observations, including the fact that in deeper horizons the water content increased very quickly after infiltration started (after only 38 min at 45 cm).

Applying moment analysis to the Br breakthrough curves, we calculated the mean resident time in the columns for Runs 3 and 5 (Schoen et al., 1999). These resident times are 13 and 11 min, respectively, and would have been more than 24 h if calculated on the basis of Darcy's law. The small difference between the two resident times may be explained by the difference in initial soil water content. The lower initial water content for Run 3 leads to higher mobile water content. The mass recovery of Br in the effluent was 67%. These observations indicate the presence of preferential flow, leading to rapid transport of solute through the undisturbed soil column.

As pointed out by Germann and Di Pietro (1996), the J-shaped increasing limb of the drainage hydrograph in Fig. 3 does not indicate a uniform wetting front arriving at the bottom of the soil column. They proposed two interpretations: (i) longitudinal dispersion of the wetting fronts in the individual flow paths, or (ii) various preferential-flow paths allowing for a wider spectrum of wetting front arrival times, thus leading to macroscopic lateral dispersion of a hypothetical uniform wetting front. The latter interpretation is preferable because of a relatively short residence times (between 3 and 32.5 min.) of the wetting fronts in the 0.66 m long soil column.

Table 4. Characteristic times of the drainage hydrographs for all rainfall events.†

Rainfall event number	q_0	t_b	t_s	t_0	t_D	T1	T2
	mm h^{-1}	min					
3	10.98	32.5	82	228	230	49.5	2
4	11.25	16	75	260	261.5	59	1.5
5	11.13	20.6	50.5	225	227.5	29.9	2.5
6	22.88	9.72	37	110	112	27.3	2
8	22.13	3	9	180	182.5	6	2.5
10	10.94	20	77	185	187	57	2
12	11.20	18.7	75	180	230	56.3	50

† t_b is the breakthrough time, t_s is the time of the steady flow rate establishment, t_D is the arrival time of the draining front at the bottom of the soil column, and t_0 is the duration of rainfall event. T1 and T2 have been calculated as the difference between t_s and t_b and the difference between t_D and t_0, respectively.

The drainage hydrographs changed after 10 infiltration experiments (Fig. 3). The initial breakthrough was as early in Run 12 as in Runs 4 and 10. T1 was as short in Run 12 as in Runs 4 and 10 (See Table 4), whereas T2 increased from 2 to 50 min from Run 10 to Run 12. Moreover, the steady outflow rate reached during Run 12 was lower than the incoming flow rate in the topsoil. Given that ponding at the soil surface was observed during Run 12, the constant flux boundary conditions probably changed to a variable pressure head condition at the soil surface. This change in boundary condition implies a greater influence of capillary effects on the moisture front arriving at the bottom of the column. The temporal evolution of the drainage hydrographs must be interpreted in terms of soil hydraulic properties changes, probably induced by macropore connectivity changes in the topsoil layer (H1) (Rousseau et al., 2004).

Preferential flow and rapid transport of solute were observed in our study. We believe that this is one of the criteria necessary for rapid particle-facilitated transport. Two other conditions must be met: (i) contaminants must bind with the particles, which suggests that their surface properties and particle size are important; (ii) particle concentration must be high enough to ensure significant transport of contaminants through the profile.

Size and Composition of Particles in the Leachates

Figures 5a and 5b show the size frequency distribution of eluted particles, expressed in volume and number percentages, respectively. Number percentages were estimated from the granulometer information assuming that all particles were spherical. This result must be interpreted with caution since natural soil particles are not spherical and this transformation remains an approximation.

As shown in Fig. 5a, the size of eluted particles ranged from 0.3 to 300 μm. The main mode of the size distribution in number percentage gives the predominant size of particles in the outflow solution, which is approximately 0.45 μm (Fig. 5b). In general, we observed that larger particles were present in the first effluent samples, after which the size distribution remained relatively constant (Fig. 5a). However, we found no differences in eluted particle sizes among the different experimental conditions. These results confirm those obtained by Jacobsen et al. (1997), Kaplan et al. (1993), and Laubel et al. (1999). According to Jacobsen et al. (1997), different kinetics control the rate at which the different particle sizes are released. The different rates could be explained

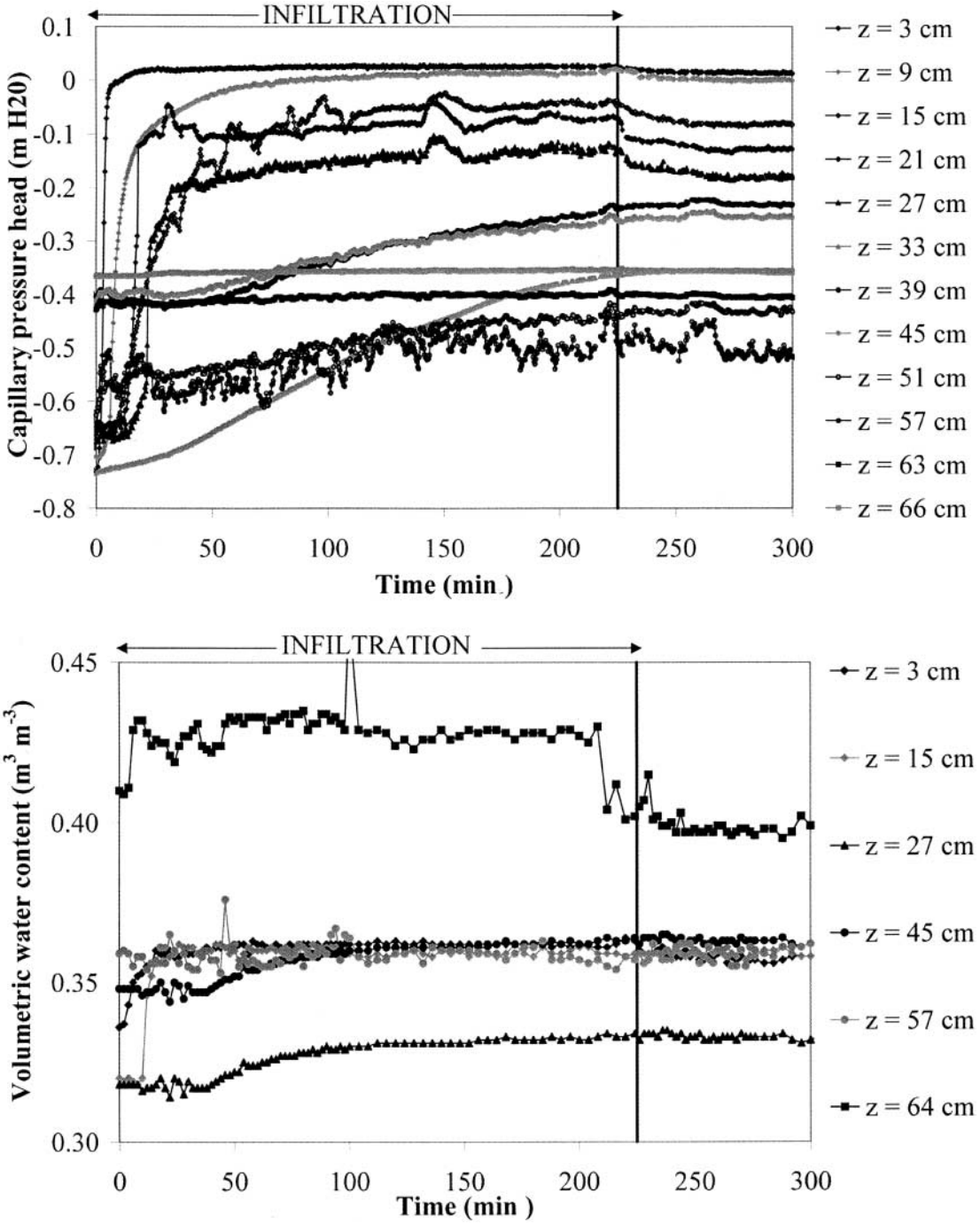

Fig. 4. (a) Tensiometer data provide capillary pressure head evolution, and (b) time domain reflectometry probes provide volumetric water content evolution during Run 5, at different depths. The beginning of infiltration experiment corresponds to $t = 0$. Data for horizon H1 are represented by diamonds, data for H2 by triangles, data for H3 by circles, and data for H4 by squares.

by the following factors: small particles are adsorbed more strongly at the macropore wall due to their relatively large surface charge, whereas large particles are more exposed to hydraulic force.

Figure 6 shows the mineralogical composition of eluted samples collected from different infiltration experiments. The eluted samples are mainly composed of smectites, which indicates that the thinnest and the permanent charged clay particles are preferentially mobilized. This means that the smectite fraction is more sensitive to ionic strength than other clays with pH-dependant charges (e.g., kaolinite and chlorite) or having high exchange capacities (e.g., illites).

The TOC content in the leachates ranged from 1.6 ± 0.2 to 19.5 ± 2.9 mg L^{-1} and was always higher at the beginning of the outflow (Fig. 7). These figures confirm the results obtained by Kaplan et al. (1993) and Worrall et al. (1999). Water input rates had an effect on the TOC content of eluted samples only at the onset of the breakthroughs: the TOC content was initially three

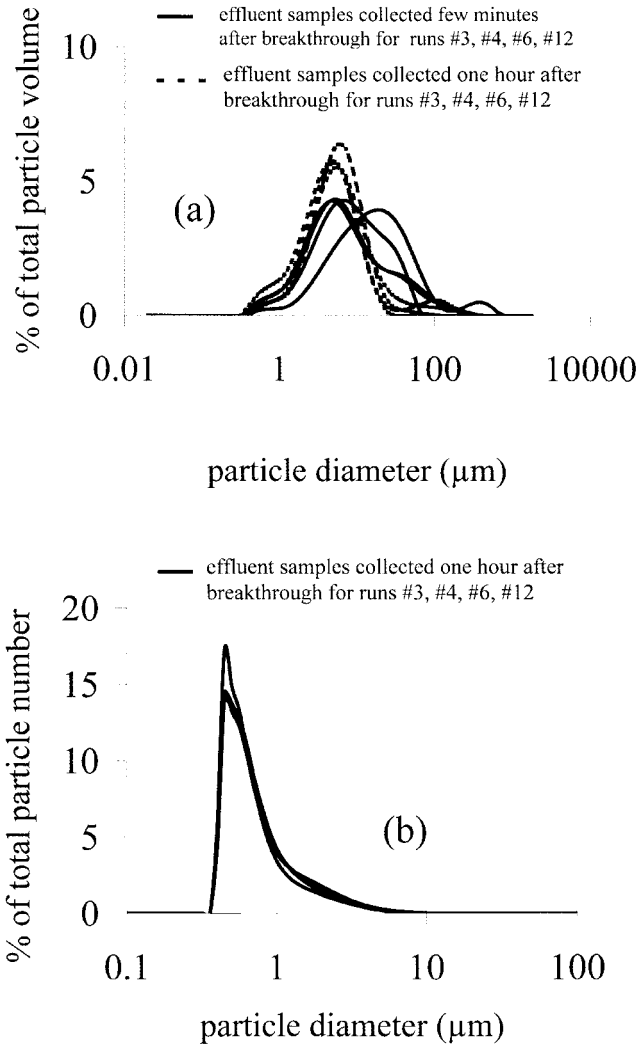

Fig. 5. Particle-size distribution measured by laser diffraction. (a) Size distribution evolution during infiltration experiments (in percentage of particle volume). The unbroken line represents the size distribution for the first effluent samples, just after breakthrough, and the dotted line is for effluent samples collected after about one hour of draining. (b) Size distribution in percentage of total number of particles.

times higher at the higher input rate (see Fig. 7a), but later became the same as those for the lower input rate.

If we accept the hypothesis of detachment by raindrop impact at the soil surface, then higher rainfall intensity should be more favorable for topsoil erosion and leaching of organic matter at the onset of the flow. On the other hand, a higher topsoil water content could make the surface more sensitive to erosion. When the initial soil moisture content is close to saturation (Fig. 7b), the mean TOC content (8.5 ± 1.3 mg L^{-1}) was higher than when the soil was at field capacity (5.5 ± 0.8 mg L^{-1}). However, no significant effect of ionic strength on the TOC content of eluted samples was observed (Fig. 7c, Table 5).

Both the effects of temporal evolution and that of the soil surface tillage on the TOC content of eluted samples are shown in Fig. 7d. The topsoil was naturally modified by erosion after each infiltration, except for Run 10, which was tilled to a depth of 2 cm just before infiltration. Successive infiltrations reduced in the mean eluted TOC content (see Table 5) due to natural changes of the soil surface. However, the mean eluted TOC content increased for Run 10. Several hypotheses may explain these observations. The first possibility is that since the topsoil is a pool of dispersible organic particles, any changes in its structure could have an impact on the eluted TOC content. In the case of natural evolution by raindrop erosion, a crust that develops in the first centimeters of the topsoil could decrease the effective mean pore size (Roulier et al., 2002), thus causing a decrease in potentially dispersible particles. On the other hand, when the topsoil has been freshly tilled, the porosity is increased and potentially dispersible particles could be increased.

The mean concentrations of Ca^{2+} and Mg^{2+} in eluted samples from each infiltration are reported in Table 5. As could be expected, the higher the Mg^{2+} concentration of the incoming solution, the higher the Mg^{2+} concentration of the outflow solution. Moreover, the higher the Mg^{2+} concentration of the incoming solution, the higher the Ca^{2+} concentration of the leachates as well. According to theory, Mg^{2+} is a cation with a larger hydration sphere than Ca^{2+}, which will induce more clay dispersion at equal salt concentrations. However, an increase in the Mg^{2+} concentration can cause an exchange with Ca^{2+}. According to the measured soil chemical properties (Table 1), all profile horizons were initially Ca-saturated, which suggests that Mg^{2+} of the infiltrating water will replace Ca^{2+} on the negative charged particles. These results indicate that chemical processes are involved, leading to changes in the chemical composition of resident pore water. Electrolyte concentration changes may have an influence on attractive and repulsive forces between soil particles, and thus on particle mobilization.

Concentration, Kinetics of Eluted Particles, and Physicochemical Effects on Particle Mobilization

For all of the infiltration experiments, the particle concentration increased at the beginning of the infiltration and decreased just after rainfall stops (Fig. 8). The concentration of eluted particles was correlated with the drainage flow intensity, particularly during transient flow. Figure 8a shows that the higher the water input rate, the higher the particle concentration in the effluent. For the higher input rate, the maximum concentration (1900 ± 95 mg L^{-1}) was nearly two times higher than for the lower input rate (850 ± 42 mg L^{-1}). The particle concentration increases quasi-linearly during low infiltration rates, whereas it was highest when the infiltration rate was high. This behavior may imply a rate-limited dynamics. The amount of available particles in the soil column was probably limited during infiltration experiments and the threshold of available particles was more rapidly reached at higher infiltration rates. The effect of infiltration rate on particle detachment was probably linked to mechanical mechanisms like shear

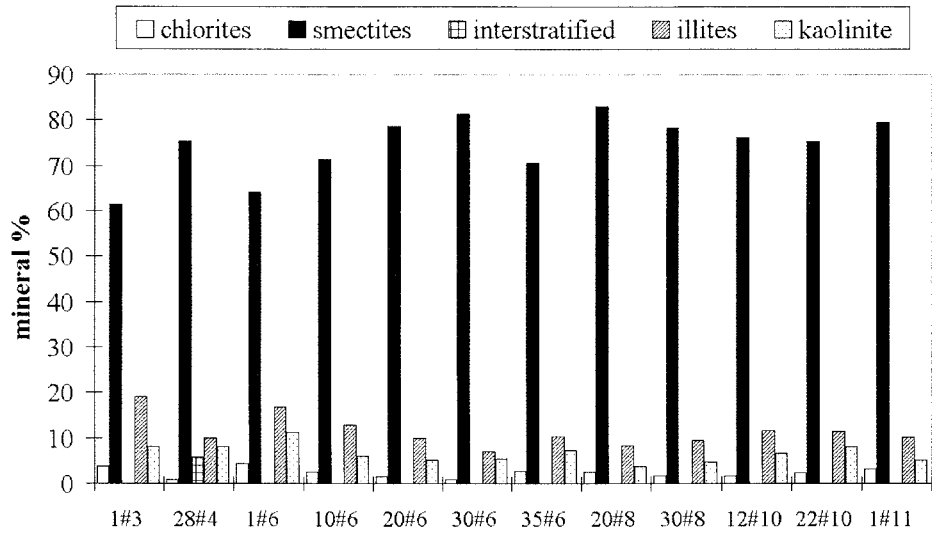

Fig. 6. Mineralogical composition of several effluent samples.

stress. Shear stress along macropore walls is positively correlated to flow velocity into macropores and is much greater at high flow rates.

We assume that chemical equilibrium was not reached between mobile pore water and resident water during transient flow. Therefore, only the water flow velocity and the initial soil water content may have affected initial mobilization rate. During steady water flow, the leaching process becomes more complex, and it varies with the involved boundary and initial conditions of the infiltration experiments.

For all experiments (except when the initial water content was close to saturation; Run 8), the particle breakthrough curve exhibited a peak in concentration at the beginning of leaching. We hypothesize that this was due to detachment by shear stress along macropore walls at the onset of the flow. Wan and Wilson (1994a, 1994b) observed that particles might sorb to an air–water interface. In a macroporous flow system, the initial mobilization rate may therefore originate from flushing of the air–water interface present before flow initiation, with the particles adhering to the interface. However, we cannot exclude the hypothesis that this peak is the result of the depositioning of some particles on the Plexiglas plate.

The wetter the soil, the higher the particle concentration in the effluent. The maximum concentration was about two times higher (3600 ± 180 mg L^{-1}) for satu-

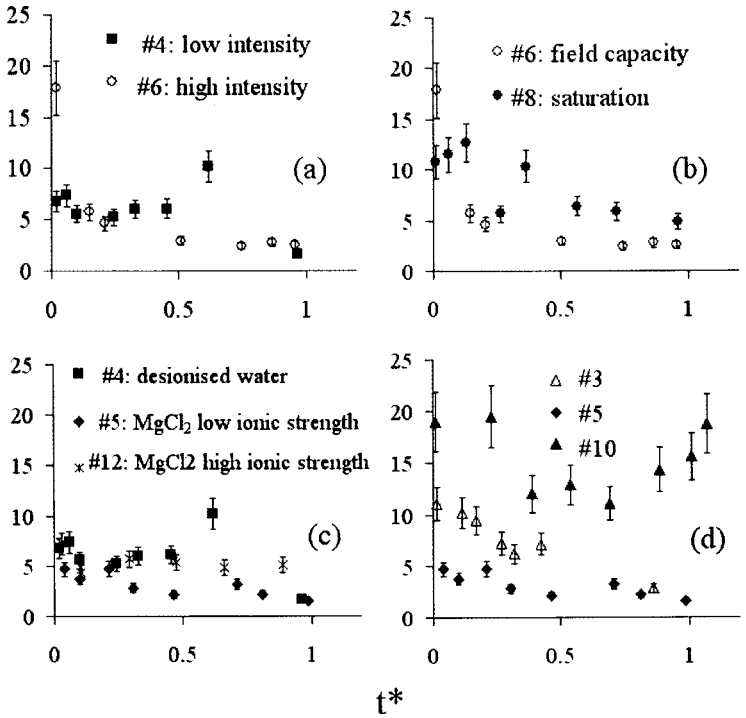

Fig. 7. Total organic C content evolution during infiltration time for all experiments: (a) as a function of rainfall intensity, (b) as a function of initial moisture content, (c) as a function of the ionic strength, and (d) as a function of temporal evolution and soil surface tillage.

Table 5. Effluent concentration in Ca^{2+} and Mg^{2+} for all rainfall events.

Rainfall event number	Mean TOC content†	Mean [Mg^{2+}]‡	Mean [Ca^{2+}]§
	mg L^{-1}		
3	7.7 ± 1.2	3.86 ± 0.08	38.8 ± 1.6
4	6.1 ± 0.9	1.60 ± 0.03	13.4 ± 0.5
5	3.1 ± 0.5	4.13 ± 0.08	19.9 ± 0.8
6	5.5 ± 0.8	2.04 ± 0.04	16.1 ± 0.6
8	8.5 ± 1.3	2.02 ± 0.04	18.4 ± 0.7
10	14.8 ± 2.2	4.72 ± 0.09	35.2 ± 1.41
12	5.4 ± 0.8	593 ± 12	290 ± 12

† Calculated from the TOC content of all of the effluent samples.
‡ Calculated from the [Mg^{2+}] of all of the effluent samples.
§ Calculated from the [Ca^{2+}] of all of the effluent samples.

rated soil than when the soil was at field capacity (Fig. 8b). Any of two processes may explain this phenomenon: (i) all macropores are not yet empty and water flow therefore occurs in both the macropores and the micropores, thus increasing the effective porosity and mechanical detachment and particle transport, and (ii) saturated conditions lead to an increase in the pressure head in the smallest pores and, as a result, an increase in the total potential of soil water, which could change the arrangement of clay particles and weaken attractive forces between soil particles (Tessier, 1991). Thus, mechanical detachment of particles needs less kinetic energy and leads to a higher initial mobilization rate. Another possible cause could be turbulent flow in the macropores and its role in the detachment of colloids. However, the Reynolds number, Re, ranged from 6.4 to 64 for Run 8 assuming macropores of about 1 mm in diameter, depending upon the macropore mobile water content (from 0.001 to 0.0001 $m^3\ m^{-3}$, respectively). The Reynolds number is defined here as $(q_0/\theta_m)d/\nu$, in which q_0 is Darcy's flux, θ_m is the macropore mobile water content, d is the diameter of macropore and ν is the kinematic viscosity. According to Schneebeli (1987), flow in a porous media becomes turbulent at about Re = 60; also, Darcy's law reaches its limit of validity at Re = 2. Maruyama (2003) found Re from 18.4 to 89.7, from which they concluded that the flow is transitional from laminar to turbulent. While turbulent flow may well have occurred in our experiments, precise data to confirm this and the exact nature of the preferential flow process are lacking.

Both the nature of the incoming solution (deionized water or $MgCl_2$) and its ionic strength (10^{-3} or 10^{-1} M)

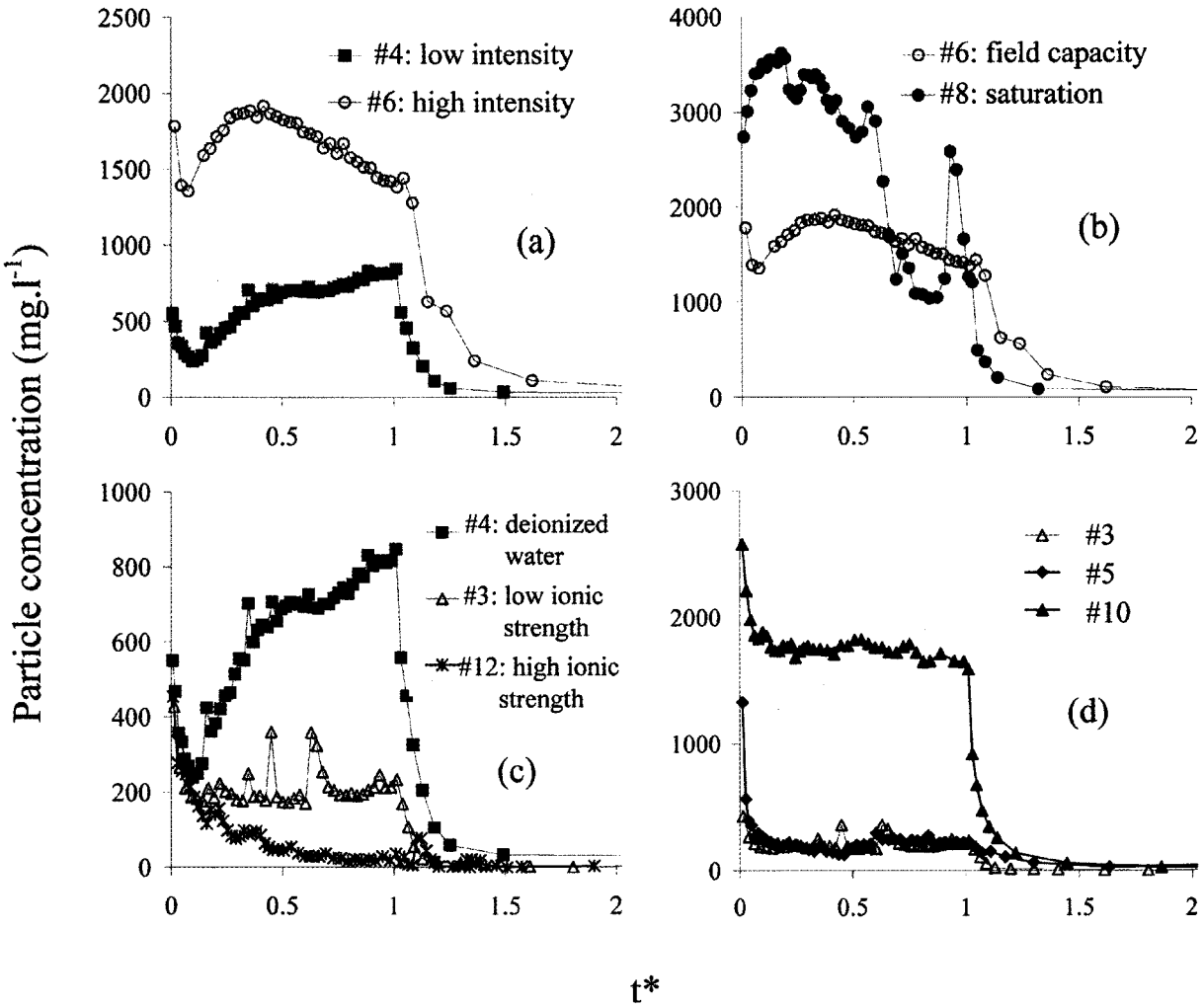

Fig. 8. Particle breakthrough curves: (a) as a function of the rainfall intensity, (b) as a function of initial moisture content, (c) as a function of the ionic strength, and (d) as a function of temporal evolution.

may have an effect on particle mobilization. The concentration of eluted particles is inversely proportional to the Mg concentration of the incoming solution and, thus, inversely proportional to the ionic strength of the solution (see Fig. 8c). When deionized water is infiltrated, the concentration of eluted particles increases during steady flow whereas when $MgCl_2$ is supplied to the soil column, it remains constant or exponentially decreases for low and high Mg^{2+} concentration, respectively. The hypothesis proposed by Fauré et al. (1996), suggesting that ionic strength acts on particle mobilization as a threshold mechanism, seems consistent with our results. Previous studies (e.g., Tessier, 1991) suggest that the threshold corresponds to an ionic strength of about 10^{-4} *M*. Furthermore, the lower the ionic strength, the higher the osmotic potential and, therefore, the higher the total potential of soil water (Miyazaki, 1993). This implies that links between soil particles become weaker, thus increasing detachment by mechanical stress (Tessier et al., 1999).

Figure 8d compares the breakthrough curves of eluted particles recorded during replications of the control experiment (see Table 2). The shapes of the leaching curves are much alike. There is a significant leaching of naturally occurring particles at the beginning of the infiltration experiments after which the concentration declines to a constant low level. However, for Exp. 10, concentration values are almost one order of magnitude higher than those for Exp. 3 and 5. A surface crust appears after Run 8 (highest water input rate) so we decided to scrape the surface before infiltration for Runs 10 to 12 to obtain similar surface initial conditions to all the experiments. However, deeper structural changes (see Fig. 1a,b and Table 3) could affect both hydraulic properties and particles mobilization. Furthermore, the decrease in the topsoil layer macroporosity probably induced dead end macropores, increasing the initial moisture content of the topsoil (Table 2) and leading to a higher particle detachment as illustrated in Fig. 8b.

Processes Involved in Particle Mobilization

A more detailed analysis of the obtained experimental data is discussed from the point of view of the cumulative mass of eluted particles versus the square root of time (Fig. 9b). Laegdsmand et al. (1999) and Jacobsen et al. (1997) observed that the cumulative mass of mobilized particles versus the square root of time exhibited a fairly linear increase after a few minutes during infiltration experiments performed on undisturbed soil columns. They hypothesized that particle mobilization was diffusion-limited in the boundary layer between grain surfaces and the bulk fluid. However, for comparable conditions of water input rates and ionic strength of the incoming solution, the cumulative mass of mobilized particles for the same period of drainage was lower in their experiments than in ours. For Exp. 8 (deionized water, high infiltration rate, saturated initial conditions), more than 10 000 mg of eluted particles were recovered from our column during 120 min of drainage whereas only 35 mg were eluted during the same period in the infiltration experiments of Jacobsen et al. (1987). Therefore, processes involved in particle mobilization must be different depending on chemical and soil structural properties, and should lead to different mobilization kinetics.

As suggested by Fig. 9a and 9b, a power law or a second-order polynomial function should be more suitable to fit the cumulative mass of mobilized particles versus the square root of time. An explanation could be that diffusion across hydrodynamic boundary layers is not the only factor limiting particle mobilization. Two kinetics can be distinguished from Fig. 9b. The initial mobilization rate is similar, regardless of the ionic strength of the incoming solution. During steady state, the cumulative mass of eluted particles versus the square root of time then exhibits different behaviors, depending on the ionic strength of incoming solution.

For Run 5, the ionic strength of incoming solution (1.6×10^{-3} *M*) was close to that of the initial soil–water system (2×10^{-2} to 7.5×10^{-3} *M*, depending on the soil layer). The kinetics of particle mobilization remained nearly identical to that of the initial stage. As a matter of fact, in the case where the ionic strength of incoming solution was the same as that of the soil–water system and there is no exchange between soil particle and solution, the energy barrier present at the soil–water interface could not be altered. Besides, the pH of the incoming solution was close to that of the initial soil–water system as well (=7) and $MgCl_2$ (neutral salt) do not induce pH variation, so that the number and type of sites could not be modified and further energy barrier could not be altered. Thus, in this case, the only limiting factor for particle mobilization was the diffusion across the hydrodynamic boundary layer (Ryan and Gschwend, 1994). In the case of Exp. 12, the ionic strength of incoming solution was one order of magnitude higher than that of the soil–water system. The cumulative mass of eluted particles versus the square root of time leveled off after the linear increase. Once the steady flow is established into the soil column, the ionic strength of the incoming solution may induce an increase in the ionic strength of the soil–water system. This results in a decrease in the size of the energy barrier, increasing aggregation forces between clay layers (Ryan and Gschwend, 1994). Mobilization may therefore be limited by particle deposition at the soil–water interface. Moreover, the Ca^{2+} occurrence in the flowing solution after cation exchange could facilitate particle flocculation and deposition, as observed by Kretzschmar and Sticher (1997) and Grolimund et al. (1998).

In the case of Run 4 (Fig. 9a,b), the ionic strength of the incoming solution is three orders of magnitude lower than that of the soil–water system. An increase in the particle mobilization rate is observed during the steady flow. The mobilization of colloids by a change in solution chemistry depends on the alteration of the forces between the surfaces of colloids and the aquifer grains to which they are attached. These intersurface forces include double diffusive layer (DDL), London–van der Waals attraction, and poorly characterized short-range non DLVO forces such as hydration and steric repulsion

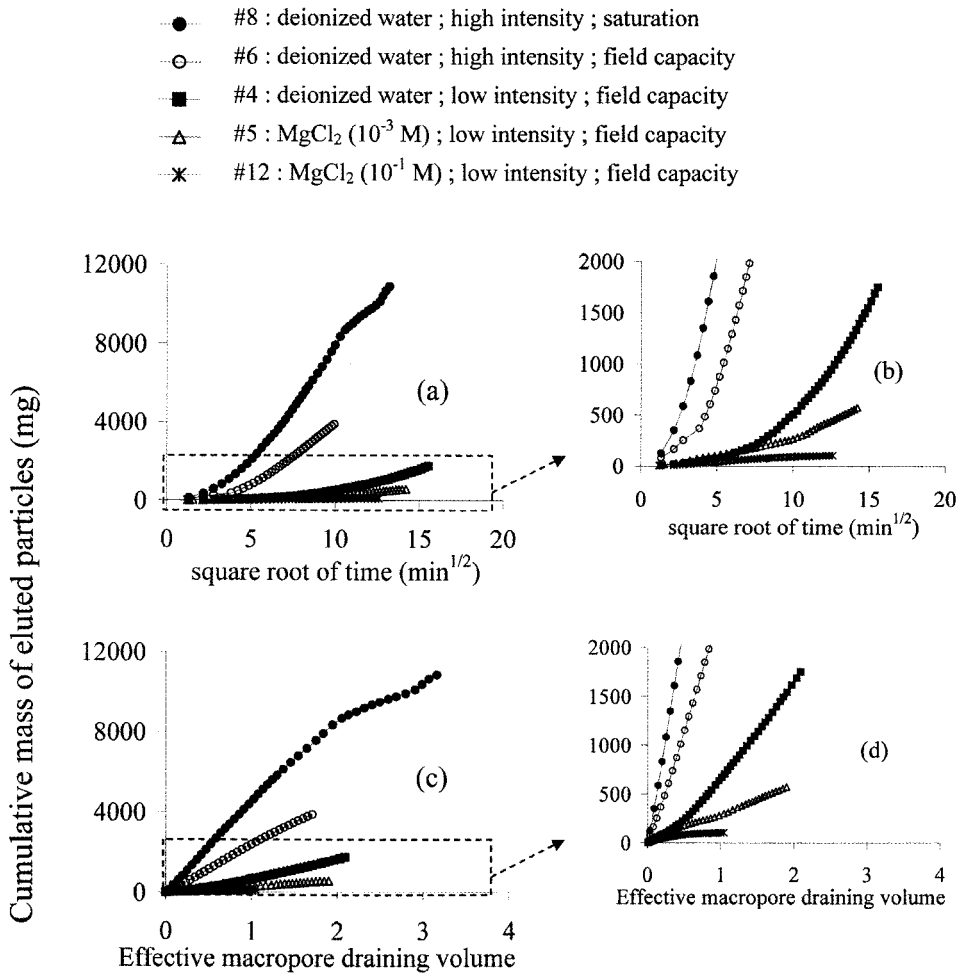

Fig. 9. (a) Cumulative mass of particles in the effluent vs. the square root of dimensionless time, for all the experiments. (b) An enlargement of (a) for cumulative mass of eluted particles ranges from 0 to 2000 mg. (c) Cumulative mass of particles in the effluent vs. draining volume expressed in effective pore volume. (d) An enlargement of (c) for cumulative mass of eluted particles ranges from 0 to 2000 mg.

(Derjaguin and Landau, 1941; Verwey and Overbeek, 1948). The decrease ionic strength and subsequent expansion of the DDL and spacing between clay particles enhances vulnerability to detachment by mild shear forces exerted by the flowing fluid.

In Fig. 9c and 9d, the cumulative mass of eluted particles is plotted versus the cumulative eluted pore volume. Figure 9c shows that a linear regression could fit the data for all experiments. This observation could confirm the experiment of El Farhan et al. (2000). The results reflect a relatively steady generation rate of soil particles, even for total infiltration rates equivalent to the expected amount of precipitation for one month at our site. However, the slopes of the linear regressions vary by several orders of magnitude, depending on the experimental conditions described earlier. Differences in slopes for different rainfall intensities suggest that factors other than different fluid residence times may be involved; and could confirm our hypothesis that macropore flow velocity and induced shear stress are involved in particle detachment.

CONCLUSIONS

This study, performed in the laboratory on a loamy clay soil column taken from a tilled soil, has shown that there is a potential for considerable leaching of naturally occurring particles at rainfall intensities corresponding to natural storm events. This suggests that there is a risk of particle transport during storms, resulting in particle-mediated transport of adsorbing contaminants. The evidence that preferential paths, and therefore preferential flow processes prevail in this soil increases the risk of groundwater pollution by rapid transport after rainfall events.

The eluted particles consist mainly of the thinnest clays with low and permanent charge (smectites) whose size is approximately 0.45 μm. Moreover, their size decreases during the leaching of naturally occurring particles as well as organic C content, probably associated to clay particles. However, the size of eluted particles and their mineralogical nature are not affected by physical and chemical changes of infiltration conditions.

We show in this experimental study that particle mobilization is most extensive at high rainfall intensities, low ionic strength and initial soil moisture content close to saturation. On the other hand, particle mobilization is limited at high ionic strength associated with the divalent cation Mg^{2+}. This is in agreement with results obtained on repacked soil samples or artificial porous media. However, both chemical and physical mechanisms

must be involved in particle mobilization, even in soils that do not contain significant amount of Na^+ or K^+ exchangeable cations. The effect of rainfall intensity on particle detachment is probably linked to such mechanical processes as shear stress along macropore walls. Furthermore, the lower the ionic strength (low salt concentration), the higher the osmotic potential and, therefore, the higher the total soil water potential. Under saturated conditions, an increase in the capillary potential in the smallest pores leads to an increase in the total potential of pore soil water. This implies that aggregation forces between soil particles become weaker and that detachment is thus enhanced by mechanical stress. According to Tessier (1991) and Touret et al. (1990), the interparticles pore space varies with cation electrolyte level, applied stresses, and the history of applied stresses. Based on a study of the major types of clay, they concluded that all properties of these systems must be related to the clay microstructure at its pore scale. For clay smectites, the behavior of the system depends primarily on interactions between layers through their hydrated interlayer cations. This behavior further depends on particle interactions in relation to the interface characteristics at the level of interparticles pores. A thorough understanding of particle mobilization requires the simultaneous consideration of all levels of clay structural organization, from the crystallographic unit level to the most macroscopic structures.

A control experiment repeated three times before and after several infiltration experiments revealed the transient nature of particle leaching after several rainfall events. A decrease in the topsoil layer macroporosity after several infiltrations experiments was demonstrated by comparison of the three-dimensional reconstructions of macropore networks. This reduction in macroporosity probably induced the creation of dead-end macropores, and increased the initial moisture content of the topsoil and leading to increased particle detachment. Further research is needed so as to incorporate our experimental findings in a realistic particle mobilization/transport model.

ACKNOWLEDGMENTS

A Doctor Engineer fellowship to Marine Rousseau by the CNRS (French National Research Centre) is thankfully acknowledged. This work was partially supported by the PNRH ("Programme National de Recherches en Hydrologie", French Hydrology Program).

REFERENCES

Artinger, R., B. Kienzler, W. Schubler, and J.I. Kim. 1998. Effects of humic substances on the ^{241}Am migration in a sandy aquifer: Column experiments with Gorleben groundwater/sediment systems. J. Contam. Hydrol. 35:261–275.

Capowiez, Y., A. Pierret, O. Daniel, P. Monestiez, and A. Kretzschmar. 1998. 3D skeleton reconstructions of natural earthworm burrow systems using CAT scan images of soil cores. Biol. Fertil. Soils 27:51–59.

Champ, D., W. Merrit, and J. Young. 1982. Potential for the rapid transport of plutonium in groundwater as demonstrated by core column studies. p. 745–754. *In* W. Lutze (ed.) Scientific basis for radioactive waste management. Vol. 5. Elsevier Science Publishing, New York.

Degueldre, C., H.R. Pfeiffer, W. Alexander, B. Wernli, and R. Bruetsch. 1996. Colloid properties in granitic groundwater systems. I: Sampling and characterisation. Appl. Geochem. 11:677–695.

Derjaguin, B.V. and L. Landau. 1941. Acta Physicochim. 14:633.

El-Farhan, Y.H., N.M. Denovio, J.S. Herman, and G.M. Hornberger. 2000. Mobilization and transport of soil particles during infiltration experiments in an Agricultural field, Shenandoah Valley, Virginia. Environ. Sci. Technol 34:3555- 3559.

Elimelech, M., and C.R. O'Melia. 1990. Kinetics of deposition of colloidal particles in porous media. Environ. Sci. Technol. 24: 1528–1536.

Fauré, M.H., M. Sardin, and P. Vitorge. 1996. Transport of clay particles and radioelements in a salinity gradient: Experiments and simulations. J. Contam. Hydrol. 21:255–267.

Gamerdinger, A.P., and D.I. Kaplan. 2001a. Physical and chemical determinants of colloid transport and deposition in water-unsaturated sand and Yucca Mountain Tuff material. Environ. Sci. Technol 35:2497–2504.

Gamerdinger, A.P., and D.I. Kaplan. 2001b. Colloid transport and deposition in water-saturated Yucca Mountain Tuff as determined by Ionic Strength. Environ. Sci. Technol 35:3326–3331.

Germann, P.F., and L. Di Pietro. 1996. When is porous-media flow preferential? A hydromechanical perspective. Geoderma. 74:1–21.

Grant, R., A. Laubel, B. Kronvang, H.E. Andersen, L.M. Svendsen, and A. Fuglsang. 1996. Loss dissolved and particulate phosphorus from arable catchments by subsurface drainage. Water Res. 30: 2633–2642.

Grolimund, D., M. Elimelech, M. Borkovec, K. Barmettler, R. Kretzschmar, and H. Sticher. 1998. Transport of in situ mobilized colloidal particles in packed soil columns. Environ. Sci. Technol. 32:3562–3569.

Gruesbeck, C., and R.E. Collins. 1982. Entrainment and deposition of fine particles in porous media. Soc. Pet. Eng. J. 22:847–856.

Hardy, I.A.J., A.D. Carter, P.B. Leeds-Harrison, I.D.L. Foster, and R.M. Sanders. 2000. The origin of sediment in field drainage water. p. 241–257. *In* I.D.L. Foster (ed.) Tracers in Geomorphology. John Wiley & Sons Ltd., New York.

Harter, T., S. Wagner, and E.R. Atwill. 2000. Colloid transport and filtration of Cryptosporidium parvum in sandy soils and aquifer sediments. Environ. Sci. Technol. 34:62–70.

Jacobsen, O.H., P. Moldrup, C. Larsen, L. Konnerup, and L.W. Petersen. 1997. Particle transport in macropores of undisturbed soil columns. J. Hydrol. (Amsterdam) 196:185–203.

Jarvis, N.J., K.G. Villholth and B. Ulen. 1999. Modelling particle mobilization and leaching in macroporous soil. Eur. J. Soil Sci. 50:621–632.

Jensen, D.L., and T.H. Christensen. 1999. Colloidal and dissolved metals in leachates from four danish landfills. Water. Res. 33: 2139–2147.

Kaplan, D.I., P.M. Bertsch, D.C. Adriano, and W.P. Miller. 1993. Soil-borne mobile colloids as influenced by water flow and organic carbon. Environ. Sci. Technol. 27:1193–1200.

Kaplan, D.I., P.M. Bertsch and D.C. Adriano. 1995. Facilitated transport of contaminant metals through an acidified aquifer. Ground Water 33:708–717.

Kaplan, D.I., M.E. Sumner, P.M. Bertsch, and D.C. Adriano. 1996. Chemical conditions conducive to the release of mobile colloids from ultisol profiles. Soil Sci. Soc. Am. J. 60:269–274.

Kaplan, I., P.M. Bertsch, and D.C. Adriano. 1997. Mineralogical and physicochemical differences between mobile and nonmobile colloidal phases in reconstructed pedons. Soil Sci. Soc. Am. J. 61:641–649.

Kretzschmar, R., W.P. Robarge, and S.B. Weed. 1993. Flocculation of Kaolinitic soil clays: Effects of humic substances and Iron Oxides. Soil Sci. Soc. Am. J. 57:1277–1283.

Kretzschmar, R., W.P. Robarge, and A. Amoozegar. 1995. Influence of natural organic matter on colloid ttransport through saprolite. Water Resour. Res. 31:435–445.

Kretzschmar, R., K. Barmettler, D. Grolimund, Y. Yan, M. Borkovec, and H. Sticher. 1997. Experimental determination of colloid deposition rates and collision efficiencies in natural porous media. Water Resour. Res. 33:1129–1137.

Kretzschmar, R., and H. Sticher. 1997. Transport of humic-coated iron oxide colloids in a sandy soil: Influence of Ca^{2+} and trace metals. Environ. Sci. Technol. 31:3497–3504.

Kretzschmar, R., M. Borkovec, D. Grolimund, and M. Elimelech. 1999. Mobile subsurface colloids and their role in contaminant transport. Adv. Agron. 66:121–193.

Laegdsmand, M., K.G. Villholth, M. Ullum, and K.H. Jensen. 1999. Processes of colloid mobilization and transport in macroporous soil monoliths. Geoderma 93:33–59.

Lanson, B. 1993. DECOMPX, X-ray Decomposition Program. Poitiers, France, ERM (Sarl).

Lanson, B. 1997. Decomposition of experimental X-ray diffraction patterns (profile fitting): A convenient way to study clay minerals. Clays Clay Miners. 45:132–146.

Laubel, A., O.H. Jacobsen, B. Kronvang, R. Grant, and H.E. Andersen. 1999. Subsurface drainage loss of particles and phosphorus from field plot experiments and a title-drained catchment. J. Environ. Qual. 28:576–584.

Maruyama, T., A. Tada, K. Iwama, and H. Horino. 2003. Direct observation of soil water movement through soil macropores using soft x-rays and stereographing. Soil Sci. 168:119–127.

McBride, M.B. 1989. Surface chemistry of soil minerals. p. 35–88. *In* J.B. Dixon and S.B. Weed (ed.) Minerals in soil environments. SSSA Book ser. 1., SSSA, Madison, WI.

McCarthy, J.F., and Zachara, J.M. 1989. Subsurface transport of contaminants. Environ. Sci. Technol. 23:496–502.

McKay, L.D., W.E. Sanford and J.M. Strong. 2000. Field-scale migration of colloidal tracers in a fractured shale saprolite. Ground Water 38:139–147.

Michel, J.C., A. Beaumont, and D. Tessier. 2000. A laboratory method for measuring the isotropic character of soil swelling. Eur. J. Soil Sci. 51:689–697.

Miyazaki, T. 1993. Water flow in soils. Marcel Dekker, New York.

Penrose, W., W. Polzer, E. Essington, D. Nelson, and K. Orlandini. 1990. Mobility of plutonium and americium through a shallow aquifer in a semiarid region. Environ. Sci. Technol 24:228–234.

Pierret, A., Y. Capowiez, L. Belzunces, and C.J. Moran. 2002. 3D reconstruction and quantification of macropores using X-ray computed tomography and image analysis. Geoderma 106:247–271.

Pilgrim, D.H., and D.D. Huff. 1983. Suspended sediment in rapid subsurface stormflow on a large field plot. Earth Surf. Proc. Landforms 8:451–463.

Roulier, S., R. Angulo-Jaramillo, L.-M. Bresson, A.-V. Auzet, J.-P. Gaudet, and T. Bariac. 2002. Water transfer and mobile water content measurement in a cultivated crusted soil. Soil Sci. 167: 201–210.

Rousseau, M., S. Ruy, R. Angulo-Jaramillo, and L. Di Pietro. 2004. Unsaturated hydraulic conductivity of structured soils from a kinematic wave approach. J. Hydraul. Res. (in press).

Roy, S.B., and D.A. Dzombak. 1996. Na^{+}–Ca^{2+} exchange effects in the detachment of latex colloids deposited in glass bead porous media. Colloids Surf. A 119:133–139.

Roy, S.B., and D.A. Dzombak. 1997. Chemical factors influencing colloid-facilitated transport of contaminants in porous media. Environ. Sci. Technol. 31:656–664.

Ryan, J.N., and P.M. Gschwend. 1990. Colloid mobilization in two coastal plain aquifers; field studies. Water Resour. Res. 26:307–322.

Ryan, J.N., and P.N. Gschwend. 1994. Effects of Ionic Strength and flow rate on colloid release: Relating kinetics to intersurface potential energy. J. Colloid Interface Sci. 164:21–34.

Ryan, J.N., and M. Elimelech. 1996. Colloid mobilization and transport in groundwater. Colloids Surf. A 107:1–56.

Saiers, J.E., and G.M. Hornberger. 1999. The influence of ionic strength on the facilitated transport of cesium by kaolinite colloids. Water Resour. Res. 35:1713–1727.

Salles, C., and J. Poesen. 2000. Rain properties controlling soil splash detachment. Hydrol. Process. 14:271–282.

Schelde, K., P. Moldrup, O.H. Jacobsen, H. de Jonge, L.W. de Jonge, and T. Komatsu. 2002. Diffusion-limited mobilization an transport of natural colloids in macroporous soil. Vadose Zone J. 1:125–136.

Schneebeli, G. 1987. Hydraulique Souterraine. Collection du Centre de recherches et d'essais de Chatou. Eyrolles, Paris.

Silliman, S. E. 1995. Particle transport through two-dimensional, saturated porous media: Influence of physical structure of the medium. J. Hydrol. (Amsterdam) 167:79–98.

Tessier, D. 1991. Behavior and microstructure of clay minerals. p. 387–415. *In* M.F. De Boodt et al. (ed.) Soil colloids and their associations in aggregates. Plenum Press, New York.

Tessier, D., F. Bigorre, and A. Bruand. 1999. La capacité d'échange: Outil de prévision des propriétés physiques des sols. (In French.) C.R. Acad. Agric. Fr. 85:37–46.

Touret, O., C.H. Pons, D. Tessier and Y. Tardy. 1990. Etude de la repartition de l'eau dans des argiles saturées Mg^{2+} aux fortes teneurs en eau. Clay Minerals 25:217–233.

Travis, B.J., and H.E. Nuttall 1985. A transport code for radiocolloid migration: With assessment of an actual low-level waste site. Mat. Res. Soc. Proc. 44:969–976.

Verwey, E.J.W. and J.T.G. Overbeek. 1948. Theory of the stability of lyophobic colloids. Elsevier, Amsterdam.

Vilks, P. and D.B. Bachinski. 1996. Colloid and suspended particle migration experiments in a granite fracture. J. Contam. Hydrol. 21:269–279.

Wan, J. and J.L. Wilson. 1994. Visualization of the role of the gas-water interface on the fate and transport of colloids in porous media. Water Resour. Res. 30:11–23.

Wan, J. and J.L. Wilson. 1994. Colloid transport in unsaturated porous media. Water Resour. Res. 30:857–864.

Wan, J. and T.K. Tokunaga. 1997. Film straining of colloids in unsaturated porous media: Conceptual model and experimental testing. Environ. Sci. Technol 31:2413–2420.

Worrall, F., A. Parker, J.E. Rae, and A.C. Johnson 1993. Suspended and colloidal matter in the leachate from lysimeters: Implications for pesticide transport and lysimeter studies. Brighton crop protection conference.

Worrall, F., A. Parker, J.E. Rae, and A.C. Johnson. 1999. A study of suspended and colloidal matter in the leachate from lysimeters and its role in pesticide transport. J. Environ. Qual. 28:595–604.